The epsilon regime with Wilson fermions

JHEP03(2009)006

(http://iopscience.iop.org/1126-6708/2009/03/006)

Published by IOP Publishing for SISSA

Received: *December 19, 2008*
Accepted: *February 4, 2009*
Published: *March 2, 2009*

The epsilon regime with Wilson fermions

Oliver Bär,[a] **Silvia Necco**[b] **and Stefan Schaefer**[a]

[a] *Institute of Physics, Humboldt University Berlin, Newtonstrasse 15, 12489 Berlin, Germany*
[b] *Instituto de Física Corpuscular, CSIC-Universitat de València, Apartado de Correos 22085, E-46071 Valencia, Spain*
E-mail: obaer@physik.hu-berlin.de, necco@ific.uv.es, sschaef@physik.hu-berlin.de

Abstract: We study the impact of explicit chiral symmetry breaking of Wilson fermions on mesonic correlators in the ϵ-regime using Wilson chiral perturbation theory (WChPT). We generalize the ϵ-expansion of continuum ChPT to nonzero lattice spacings for various quark mass regimes. It turns out that the corrections due to a nonzero lattice spacing are highly suppressed for typical quark masses of the order $a\Lambda_{\rm QCD}^2$. The lattice spacing effects become more pronounced for smaller quark masses and lead to non-trivial corrections of the continuum ChPT results at next-to-leading order. We compute these corrections for the standard current and density correlation functions. A fit to lattice data shows that these corrections are small, as expected.

Keywords: Lattice QCD, Chiral Lagrangians

ArXiv ePrint: 0812.2403

doi:10.1088/1126-6708/2009/03/006

JHEP03(2009)006

Contents

JHEP03(2009)006

1 Introduction

The ϵ-regime of QCD [1, 2] offers various advantages for the numerical determination of the low-energy couplings (LECs) in chiral perturbation theory (ChPT), the low-energy effective theory of QCD. Only the leading order LECs, the pseudo scalar decay constant in the chiral limit F and the chiral condensate Σ, enter the predictions of ChPT through next-to-leading order (NLO) in the epsilon expansion. The Gasser-Leutwyler coefficients [3, 4] first appear at one order higher, thus making the ϵ-regime attractive for precise determinations of F and Σ.[1] In addition, gauge field topology plays an important role in the ϵ-regime [6]. ChPT makes predictions for correlation functions restricted to individual topological sectors, thus enlarging the number of observables that can be compared to numerical lattice QCD results.

The role of topology and spontaneous chiral symmetry breaking has led to the widespread conviction that overlap [7] or domain-wall fermions [8–10] are the preferred or even mandatory choice for lattice simulations in the ϵ-regime. Consequently, a fairly large number of quenched simulations with these fermions in the ϵ-regime can be found in the literature [11–19]. Even though the results were to a large extend promising, the main hurdle for progress in real QCD is the need for simulations with dynamical sea quarks, and these are extremely time-consuming.[2] So far only the JLQCD collaboration [21] has carried out a large scale dynamical simulation with overlap fermions in the ϵ-regime, and the computer resources that went into this simulation are enormous.

In contrast, fairly inexpensive simulations with tree-level improved Wilson fermions have been reported recently [22]. Reweighting as described in ref. [23] has been used to reach small enough quark masses in order to be in the ϵ-regime. The size of the box was $L \simeq 2.8$fm, much larger than in all the simulations mentioned before. Quite surprisingly, the data for the axial vector and pseudo scalar correlation functions are very well described by the corresponding ChPT predictions, although chiral symmetry is explicitly broken for Wilson fermions.

A similar observation has been made before by the ETM collaboration [24, 25]. Their data[3], obtained with a twisted mass term [27, 28], also suggests that the ϵ-regime can be reached with Wilson fermions. One might argue that automatic $\mathrm{O}(a)$ improvement at maximal twist [29–31] may suppress chiral symmetry breaking effects. Still, the data obtained with Wilson fermions raises the question if and how the results can be interpreted in the presence of the explicit chiral symmetry breaking by the Wilson term.

In this paper we study this question with Wilson ChPT [32, 33], the low-energy effective theory for lattice QCD with Wilson fermions. And indeed, our analysis suggests a natural answer to the question raised above. It turns out that the lattice spacing corrections are in general highly suppressed and show up at higher order in the epsilon expansion. For example, for quark masses $m \sim a\Lambda_{\mathrm{QCD}}^2$ the deviations from the continuum results due to the $\mathrm{O}(a)$ corrections enter first at next-to-next-to-leading order (NNLO). This is in contrast to the expansion in the p-regime, where the corrections already appear at next-to-leading

[1] For a recent review of the various estimates see [5].
[2] For a recent review see [20].
[3] A review of the ETM results can be found in ref. [26].

JHEP03(2009)006

order. This suppression is completely analogous to the suppression of terms involving the Gasser-Leutwyler coefficients in continuum ChPT in the ϵ-regime.

However, the power counting in WChPT can be different, depending on the relative size of the quark mass m and the lattice spacing a. For this reason we also consider a different power counting where $m \sim a\Lambda_{\rm QCD}^2$ is no longer appropriate. In this case the lattice spacing corrections enter already at NLO. Interestingly, these corrections are entirely caused by the $\mathrm{O}(a^2)$ term in the chiral effective Lagrangian that also determines the phase diagram of the lattice theory [32]. The corrections linear in the lattice spacing, stemming from the effective Lagrangian and the effective operators, are still of higher order in the epsilon expansion. This is relevant in practice: The Wilson ChPT expressions contain only one more unknown LEC at this order, and the predictive power is not spoiled by a plethora of free fit parameters.

We also use our WChPT results derived here for an analysis of the data of ref. [22]. The corrections due to the nonzero lattice spacing turn out to be very small, supporting our theoretical analysis that these corrections are in general highly suppressed. This is very encouraging for lattice simulations with Wilson fermions. The impact of explicit chiral symmetry breaking for ϵ-regime simulations is much less severe than previously thought. This makes simulations with Wilson fermions a serious and efficient alternative to those with chiral fermions.

2 Wilson chiral perturbation theory (WChPT)

2.1 Chiral Lagrangian

The chiral effective Lagrangian of WChPT is expanded in powers of (small) pion momenta p^2, quark masses m and the lattice spacing a. Based on the symmetries of the underlying Symanzik action [34, 35] the chiral Lagrangian including all terms of $\mathrm{O}(p^4, p^2m, m^2, p^2a, ma)$ is given in ref. [33]. The $\mathrm{O}(a^2)$ contributions are constructed in ref. [36] and, independently, in ref. [37] for the two-flavor case.

In the following we will restrict ourselves to $N_f = 2$ with degenerate quark mass m. The continuum part of the chiral Lagrangian is the well-known Gasser-Leutwyler Lagrangian [3, 38]. With our notations the leading part reads (in Euclidean space-time)

$$\mathcal{L}_2 = \frac{F^2}{4}\mathrm{Tr}\left(\partial_\mu U \partial_\mu U^\dagger\right) - \frac{F^2 B}{2} m \mathrm{Tr}\left(U + U^\dagger\right). \tag{2.1}$$

The field U containing the pion fields is defined as usual,

$$U(x) = \exp\left(\frac{2i}{F}\xi(x)\right), \qquad \xi(x) = \xi^a(x) T^a. \tag{2.2}$$

The SU(2) generators are normalized such that $\mathrm{Tr}(T^a T^b) = \delta^{ab}/2$, so $T^a = \sigma^a/2$ in terms of the standard Pauli matrices σ^a. The coefficients B and F are the familiar leading order (LO) low-energy coefficients.[4] Higher order terms are collected in the next-to-leading order Lagrangian $\mathcal{L}_4$ [3], which we do not need in this work.

[4] With our normalization the pion decay constant in the chiral limit is $F \approx 93$MeV.

The terms involving the lattice spacing are as follows:[5]

$$\mathcal{L}_a = \hat{a}W_{45}\mathrm{Tr}\left(\partial_\mu U\partial_\mu U^\dagger\right)\mathrm{Tr}\left(U+U^\dagger\right) - \hat{a}\hat{m}W_{68}\Big(\mathrm{Tr}\left(U+U^\dagger\right)\Big)^2, \tag{2.3}$$

$$\mathcal{L}_{a^2} = \frac{F^2}{16}c_2a^2\Big(\mathrm{Tr}\left(U+U^\dagger\right)\Big)^2. \tag{2.4}$$

W_{45}, W_{68} are LECs, similar to Gasser-Leutwyler coefficients in $\mathcal{L}_4$. The quark mass and lattice spacing enter through the combinations

$$\hat{m} = 2Bm\,, \qquad \hat{a} = 2W_0a\,, \tag{2.5}$$

where W_0 is another low-energy coefficient [33]. Its presence here is for dimensional reasons: W_0 is of dimension three and $\hat{a}$ therefore of dimension two. Hence, $\hat{a}$ has the same dimension as the familiar combination Bm.

We have chosen to parametrize the $\mathrm{O}(a^2)$ contribution in terms of the LEC c_2. This coefficient plays a prominent role since its sign determines the phase diagram of the theory [32]. We briefly come back to this after we have discussed the power counting in WChPT in section 2.3.

Note that the mass parameter m in eq. (2.1) is the so-called *shifted mass* [32]. Besides the dominant additive mass renormalization proportional to $1/a$ it also contains the leading correction of $\mathrm{O}(a)$. Consequently, the term $F^2\hat{a}\mathrm{Tr}\left(U+U^\dagger\right)/4$ is not explicitly present in the chiral Lagrangian since it is absorbed in the shifted mass [33]. Of course, physical results expressed by observables do not depend on what mass is used for the parametrization of the chiral Lagrangian.

2.2 Currents and densities

The expressions for the currents and densities in continuum ChPT are well known. For example, the LO expressions for the axial vector current and the pseudo scalar density read

$$A^a_{\mu,\mathrm{ct}} = i\frac{F^2}{2}\mathrm{Tr}\left(T^a(U^\dagger\partial_\mu U - U\partial_\mu U^\dagger)\right)\,, \tag{2.6}$$

$$P^a_{\mathrm{ct}} = i\frac{F^2B}{2}\mathrm{Tr}\left(T^a(U-U^\dagger)\right)\,. \tag{2.7}$$

In WChPT these expressions receive corrections proportional to the lattice spacing. The currents and densities in WChPT can be constructed by a standard spurion analysis, similarly to the construction of the chiral Lagrangian. One first writes down the most general current/density that is compatible with the symmetries using the chiral field U, its derivatives and the spurion fields. Then, in a second step, one imposes the appropriate Ward identities valid in the theory. For the vector and axial vector current this has been done in [40]. Alternatively one can introduce source terms for the currents and densities and constructs the generating functional, as has been done in ref. [39]. Carrying over the notation of this reference the axial vector current including the leading corrections of $\mathrm{O}(a)$ reads

$$A^a_{\mu,\mathrm{WChPT}} = A^a_{\mu,\mathrm{cont}}\left(1+\frac{4}{F^2}\hat{a}W_{45}\mathrm{Tr}\left(U+U^\dagger\right)\right) + 2\hat{a}W_{10}\partial_\mu\mathrm{Tr}\left(T^a(U-U^\dagger)\right)\,. \tag{2.8}$$

[5] We essentially adopt the notation of refs. [39] and [31].

This axial vector does not satisfy any specific renormalization condition. Imposing a particular renormalization condition leads to a finite renormalization. Explicitly, one introduces [40]

$$A^a_{\mu,\mathrm{ren}}(x) = Z_A A^a_{\mu,\mathrm{WChPT}}(x) \tag{2.9}$$

with a renormalization factor Z_A.[6] Now one can impose a renormalization condition and demands that it is satisfied by $A^a_{\mu,\mathrm{ren}}$; this determines Z_A. For instance, in ref. [40] the massless chiral Ward identity has been imposed.

Quite generally, Z_A has the form (up to $\mathrm{O}(a)$)

$$Z_A = 1 + \frac{16}{F^2}\hat{a}W_A \tag{2.10}$$

with an unknown coefficient W_A. This form reflects the fact that, by construction, the WChPT current reduces to the correct continuum current for $a \to 0$. Consequently, Z_A is equal to one in the continuum limit, and (2.10) is the leading generalization for $a \neq 0$. Hence, the general form of the renormalized current is, up to $\mathrm{O}(a)$,

$$\begin{aligned} A^a_{\mu,\mathrm{WChPT}} = A^a_{\mu,\mathrm{cont}} \left(1 + \frac{4}{F^2}\hat{a}\left[W_{45}\mathrm{Tr}\left(U + U^\dagger\right) + 4W_A\right]\right) \\ +2\hat{a}W_{10}\partial_\mu \mathrm{Tr}\left(T^a(U - U^\dagger)\right). \end{aligned} \tag{2.11}$$

For brevity we have dropped the subscript "ren" on the left hand side. Terms of $\mathrm{O}(am, a^2)$ will be present at higher order in the chiral expansion.

Analogously, we use the expression [39]

$$P^a_{\mathrm{WChPT}} = P^a_{\mathrm{Cont}} \left(1 + \frac{4}{F^2}\hat{a}\left[W_{68}\mathrm{Tr}\left(U^\dagger + U\right) + 4W_P\right]\right) \tag{2.12}$$

for the pseudo scalar density. The contribution involving the LEC W_P (not present in ref. [39]) stems from a general renormalization factor $Z_P = 1 + 16\hat{a}W_P/F^2$, which we also allow, even though the results derived in this paper will not depend on the details of the $\mathrm{O}(a)$ correction.

2.3 Power counting in infinite volume

In WChPT there are two parameters that break chiral symmetry explicitly, the quark mass m and the lattice spacing a. The power counting is determined by the relative size of these two parameters.

The literature [39, 41] distinguishes two quark mass regimes with different power countings: (i) the GSM regime[7] where $m \sim a\Lambda^2_{\mathrm{QCD}}$ and (ii) the Aoki regime where $m \sim a^2\Lambda^3_{\mathrm{QCD}}$. A priori one does not know in which regime one actually has performed a simulation. For this to decide one has to compare with the predictions of WChPT and check which expressions fit the data better. However, recalling how lattice simulations are typically done one

[6] Z_A is a renormalization factor in the effective theory and should not be confused with Z_A in the underlying lattice theory.

[7] GSM stands for *generically small masses*.

can easily imagine that one starts in the GSM regime and by lowering the quark mass at fixed lattice spacing one will eventually enter the Aoki regime.

Depending on the particular regime, the LO Lagrangian is different. Since $m \sim a^2\Lambda_{\rm QCD}^3$ in the Aoki regime, also the $\mathcal{L}_{a^2}$ part in (2.4) counts as LO [37]:

$$\begin{aligned} \text{GSM regime}: \quad & \mathcal{L}_{\rm LO} = \mathcal{L}_2\,, \\ \text{Aoki regime}: \quad & \mathcal{L}_{\rm LO} = \mathcal{L}_2 + \mathcal{L}_{a^2}\,. \end{aligned}$$

The effects due to a nonzero lattice spacing are much more pronounced in the Aoki regime. Non-trivial phase transitions become relevant [32] and additional chiral logarithms proportional to a^2 appear at one loop [37, 42].

2.4 The pion mass and the PCAC mass in infinite volume

It is useful to derive the pion mass and PCAC mass at LO.

We start with the calculation of the pion mass. Expanding the LO chiral Lagrangian to quadratic order in the pion fields we obtain

$$\text{GSM regime}: \quad M_0^2 = 2Bm\,, \tag{2.13}$$

$$\text{Aoki regime}: \quad M_0^2 = 2Bm - 2c_2a^2\,. \tag{2.14}$$

The sign of c_2 determines the phase diagram of the theory [32].[8] For $c_2 > 0$ there exists a second-order phase transition separating the Aoki phase [43]. The charged pions are massless in this phase due to the spontaneous breaking of the flavor symmetry. The pion mass vanishes at $m = c_2a^2/B$. For even smaller values of m the charged pions remain massless, while the neutral pion becomes massive again [32].

Negative values of c_2, on the other hand, imply a first order phase transition with a minimal non-vanishing pion mass. All three pions are massive for all quark masses, and the pion mass assumes its minimal value at $m = 0$, resulting in

$$M_{0,\rm min}^2 = 2|c_2|a^2\,. \tag{2.15}$$

Note that magnitude and the sign of c_2 are a priori unknown and depend on the details of the underlying lattice theory, i.e. what particular lattice action has been used.

The PCAC quark mass is defined by the ratio (no sum over a)

$$m_{\rm PCAC} = \frac{\langle \partial_\mu A_\mu^a(x) P^a(0)\rangle}{2\langle P^a(x)P^a(0)\rangle}\,, \tag{2.16}$$

where angled brackets indicate expectation values. Expanding the current and the density in eqs. (2.11) and (2.12) to $\mathrm{O}(\xi^a)$ we find

$$A_\mu^a(x) = -iF\partial_\mu\xi^a(x)\,(1 + ac_A)\,, \tag{2.17}$$

$$P^a(x) = iFB\xi^a(x)\,(1 + ac_P)\,. \tag{2.18}$$

[8] Note that our definition for c_2 differs by a factor F^2a^2 from the one in ref. [32].

where here and in the following we for simplicity no longer write the subscript "WChPT". We also introduced the short hand notation

$$c_A = \frac{16}{F^2} 2W_0[W_{45} + W_A - W_{10}/4]\,, \tag{2.19}$$

$$c_P = \frac{16}{F^2} 2W_0[W_{68} + W_P]\,, \tag{2.20}$$

for the combinations of LECs in the effective current and density at this order. The correlation functions in (2.16) are now easily computed at LO, yielding

$$m_{\rm PCAC} = \frac{M_0^2}{2B}\Big(1 + a(c_A - c_P)\Big)\,. \tag{2.21}$$

Using the tree-level pion mass obtained above we find

$$\text{GSM regime}: \qquad m_{\rm PCAC} = m\Big(1 + a(c_A - c_P)\Big)\,, \tag{2.22}$$

$$\text{Aoki regime}: \qquad m_{\rm PCAC} = \Big(m - \frac{c_2}{B}a^2\Big)\Big(1 + a(c_A - c_P)\Big)\,. \tag{2.23}$$

In the GSM regime the result is rather simple and the PCAC mass is equal to the shifted quark mass, up to corrections of $\mathrm{O}(ma)$. This is no longer true in the Aoki regime. Still, the contribution proportional to $(c_A - c_P)$ is subleading and can be ignored if one works to leading order in the quark mass.

Equations (2.22) and (2.23) allow to replace the shifted mass m, which is just a parameter in the chiral Lagrangian, with the PCAC quark mass. The latter is an observable which is often used in lattice simulations.

Note that the results above reproduce a well-known fact, namely that the PCAC mass depends on the particular renormalization conditions imposed on the axial vector current and the pseudo scalar density. Different renormalization conditions show up as different values for c_A and c_P.

3 WChPT in the epsilon regime

3.1 Continuum ChPT in finite volume

Consider continuum QCD with N_f degenerate quark masses in a hypercubic volume $V = TL^3$, with $T, L \gg 1/\Lambda_{\rm QCD}$. Finite-size effects can be systematically studied by means of the corresponding chiral effective theory [1, 2, 44]. In this section we summarize the main aspects of finite-volume chiral perturbation theory in the continuum.

If the pion Compton wavelength is much smaller than the size of the box, $M_\pi L \gg 1$, finite-volume effects can be treated in the chiral effective theory by adopting the standard p-expansion, where the power-counting in terms of the momentum p is given by

$$m \sim O(p^2), \quad 1/L,\ 1/T\,, \partial_\mu \sim O(p), \quad \xi \sim O(p). \tag{3.1}$$

For asymptotically large volumes, one expects the finite-volume effects to be exponentially suppressed by factors $\sim e^{-M_\pi L}$.

On the other hand, approaching the chiral limit by keeping $\mu = m\Sigma V \lesssim O(1)$ (but still $L \gg 1/\Lambda_{\rm QCD}$), where $\Sigma = F^2 B$ is the quark condensate in the chiral limit, one explores the domain where the pion wavelength is larger than the size of the box, $M_\pi L < 1$. In this case the pion zero-mode gives a contribution to the propagator proportional to $1/M_0^2 V$, which cannot be treated perturbatively but has to be computed exactly [1, 2]. This is achieved by factorizing the pseudo Nambu-Goldstone boson fields as

$$U(x) = \exp\left(\frac{2i}{F}\xi(x)\right) U_0\,, \tag{3.2}$$

where the constant $U_0 \in \mathrm{SU}(N_f)$ represents the collective zero-mode. The nonzero modes parametrized by ξ, on the other hand, can still be treated perturbatively and satisfy the condition

$$\int_V d^4x\, \xi(x) = 0, \tag{3.3}$$

since the constant mode has been separated.

The zero-mode contribution proportional to $1/M_0^2 V$ in the pion propagator diverges in the chiral limit and a reordering of the perturbation series that sums all graphs with an arbitrary number of zero-mode propagators is necessary [2]. This reordering is achieved with the power counting

$$m \sim O(\epsilon^4), \quad 1/L,\ 1/T\,, \partial_\mu \sim O(\epsilon), \quad \xi \sim O(\epsilon). \tag{3.4}$$

Mass effects are suppressed compared to the p-regime, while volume effects are enhanced and become polynomial in $(FL)^{-2}$. Since M_0^2 is proportional to m the combination $1/M_0^2 V$ now counts as ϵ^0. Consequently, all graphs that exclusively involve zero-mode propagators count as O(1) and are unsuppressed. The key point here is, that the counting of the quark mass is dictated by the counting of L by demanding $1/M_0^2 V = \mathrm{O}(\epsilon^0)$. We will use this in the next section in order to establish the counting rules in WChPT.

With the factorization given in eq. (3.2), the leading order continuum partition function in the ϵ-regime is given by

$$Z = \int_{\mathrm{SU}(N_f)} [dU_0] \int [d\xi] \exp\left\{\frac{1}{2}\int_V d^4x \mathrm{Tr}(\partial_\mu \xi \partial_\mu \xi) + \frac{m\Sigma V}{2}\mathrm{Tr}(U_0 + U_0^\dagger)\right\}. \tag{3.5}$$

The integration over the perturbative degrees of freedom $[d\xi]$ gives rise to the usual Wick contractions, while the zero-mode integrals over $[dU_0]$ must be computed exactly. Notice that by going to $O(\epsilon^2)$, by factoring out the constant zero-mode from the measure, one obtains

$$[dU] = [d\xi][dU_0]\left(1 + A(\xi) + O(\epsilon^4)\right), \tag{3.6}$$

with

$$A(\xi) = -\frac{2N_f}{3F^2}\frac{1}{V}\int_V d^4x\, \mathrm{Tr}(\xi^2(x)) \tag{3.7}$$

for a general value of N_f [2, 45].

3.2 Power countings for the epsilon regime in WChPT

Like the continuum effective theory, WChPT can also be formulated in a finite volume, in particular the ϵ-regime discussed in this section.

In WChPT we have additional low-energy constants and the lattice spacing as an additional expansion parameter. The main task is to decide how to count these in the epsilon expansion.

Just as the continuum LECs F and Σ, we count all the additional LECs associated with the lattice spacing to be of order ϵ^0,

$$c_2, c_A, c_P \sim \mathrm{O}(1). \tag{3.8}$$

The counting of the lattice spacing a is more complicated. The general strategy is to follow the infinite-volume procedure and determine the power counting depending on the relative size of m and a. At finite volume, once the counting of m is fixed by the counting of L, we obtain the counting of a.

We start with the GSM regime. The LO Lagrangian and the pion mass M_0^2 are as in the continuum ϵ-regime, so we conclude $m \sim \mathrm{O}(\epsilon^4)$ by the same arguments as in the previous section. Since the GSM regime is defined by $m \sim a\Lambda_{\mathrm{QCD}}^2$ we are immediately lead to $a \sim \mathrm{O}(\epsilon^4)$.

The Aoki regime is more subtle. According to our assumption, the pion mass M_0^2, given in (2.14), is now a sum of two terms of equal order. If $c_2 < 0$, it is a sum of two positive terms. Hence, a small pion mass of order $\mathrm{O}(\epsilon^4)$ implies that both terms, $2Bm$ and $2|c_2|a^2$ are small too and also of order $\mathrm{O}(\epsilon^4)$.

If c_2 is positive, the pion mass is the difference of two positive contributions. This leaves the possibility that M_0^2 is small, even though the individual terms $2Bm$ and $2|c_2|a^2$ may not be small and only their difference is. A pion mass of order ϵ^4 may be obtained by the difference of two order ϵ^2 or ϵ^3 terms, for example.

We do not think that this is a likely scenario. Present day lattice simulations are usually done with small lattice spacings less than 0.1 fm and the $\mathrm{O}(a^2)$ corrections are expected to be small in this case. Hence, we *assume* that $a^2 \sim \mathrm{O}(\epsilon^4)$ in the Aoki regime. This assumption, together with the requirement $M_0^2 \sim \mathrm{O}(\epsilon^4)$ then also leads to $m \sim \mathrm{O}(\epsilon^4)$, the same counting as for $c_2 < 0$.

The epsilon expansion allows us to introduce yet another regime where we count $a \sim \epsilon^3$. Just by the powers of ϵ this is an intermediate regime between the GSM and Aoki regime. One may think about it as the GSM regime but at a larger lattice spacing (or smaller quark mass). Its usefulness will become clear in the next section when we discuss the epsilon expansion of correlation functions.

All three countings we introduced are well defined and are appropriate for a particular relative size between m and a. In order to be able to refer to these regimes we introduce the following nomenclature:

$$\begin{aligned} \text{GSM regime}: &\qquad a \sim \mathrm{O}(\epsilon^4)\,, \\ \text{GSM}^* \text{ regime}: &\qquad a \sim \mathrm{O}(\epsilon^3)\,, \\ \text{Aoki regime}: &\qquad a \sim \mathrm{O}(\epsilon^2)\,. \end{aligned} \tag{3.9}$$

JHEP03(2009)006

For fixed values of m and a in a given regime, one can match for instance the time-dependence of current correlators with lattice QCD results in order to extract the corresponding LECs.

We stress that one a priori does not know which power counting to use in analyzing numerical lattice data. For this to decide one has to analyze the data with the WChPT results for different power countings and see which one describes the data.

3.3 Epsilon expansion of correlation functions

We will be interested in correlators of the pseudo scalar density and the axial vector current. These correlators have been calculated before through NNLO in continuum ChPT [45]. In powers of ϵ this corresponds to $O(\epsilon^4)$ for the $\langle P^a(x)P^a(0)\rangle$ correlator and $O(\epsilon^8)$ for $\langle A^a_\mu(x)A^a_\mu(0)\rangle$.

In order to discuss the epsilon expansion in WChPT let us split an arbitrary operator and the action in WChPT into the continuum part and a remainder proportional to powers of a,

$$O(x) = O_{\rm ct}(x) + \delta O(x)\,, \tag{3.10}$$

$$S = S_{\rm ct} + \delta S\,. \tag{3.11}$$

Expectation values are generically defined as

$$\langle O\rangle = \frac{1}{Z}\int [dU] e^{-S} O, \tag{3.12}$$

where Z is the partition function

$$Z = \int [dU] e^{-S}. \tag{3.13}$$

The two-point correlator $\langle O_1(x)O_2(0)\rangle = \langle O_1 O_2\rangle$ (for notational simplicity we suppress the dependence on x) can then be written according to

$$\langle O_1 O_2\rangle_W = \langle O_{1,\rm ct} O_{2,\rm ct}\rangle + \delta\langle O_1 O_2\rangle\,, \tag{3.14}$$

$$\delta\langle O_1 O_2\rangle = \langle O_{1,\rm ct}\delta O_2 + \delta O_1 O_{2,\rm ct}\rangle - \langle O_{1,\rm ct} O_{2,\rm ct}\delta S\rangle + \langle O_{1,\rm ct} O_{2,\rm ct}\rangle\langle\delta S\rangle\,. \tag{3.15}$$

Here we have approximated $\exp(-\delta S) \approx 1 - \delta S$ and we dropped all higher corrections. Note that the expectation value on the left hand side of (3.14), labelled with a subscript "W", is defined with the full action S in the Boltzmann factor, while on the right hand side it is defined with $S_{\rm ct}$ only (for notational simplicity we suppress a subscript "ct").

The discretization corrections for the pseudo scalar and the axial vector can be read off from (2.11) and (2.12). For what matters here we can simplify these expressions. We are interested in the power counting for the epsilon expansion, and for this we can ignore all constants which count as O(1). Therefore, we write

$$\delta P^a \propto a\Big(\mathrm{Tr}\left(U + U^\dagger\right) + 1\Big) P^a_{\rm ct}\,. \tag{3.16}$$

δP^a is proportional to the continuum density itself. As mentioned before, the epsilon expansion of $P^a_{\rm ct}$ starts with $\mathrm{O}(\epsilon^0)$. The "scalar density" $\mathrm{Tr}(U+U^\dagger)$ also starts at $\mathrm{O}(\epsilon^0)$. Hence, by considering the continuum contribution at LO, the leading correction in the epsilon expansion due to lattice terms is completely determined by how we count the lattice spacing a. In the last section we defined three different countings, so for now we leave it unspecified, write $a \sim \epsilon^{n_a}$ where n_a counts the epsilon powers for a, and obtain

$$\delta P^a \sim \epsilon^{n_a}. \tag{3.17}$$

Note that the symbol $\sim$ stands here just for the leading lattice contribution in the epsilon expansion.

Analogously, we find for the axial vector (dropping again irrelevant constants)

$$\delta A^a_\mu \propto a\left[\left(\mathrm{Tr}\left(U+U^\dagger\right)+1\right)A^a_{\mu,\rm ct}+\partial_\mu \mathrm{Tr}\left(T^a(U-U^\dagger)\right)\right]. \tag{3.18}$$

Both, $A^a_{\mu,\rm ct}$ and $\partial_\mu \mathrm{Tr}\left(T^a(U-U^\dagger)\right)$ have an open Lorentz index and, therefore, contain at least one derivative acting on at least one power of $\xi(x)$. Hence, their continuum epsilon expansion starts at $\mathrm{O}(\epsilon^2)$ and we find for the leading lattice corrections

$$\delta A^a_\mu \sim \epsilon^{n_a+2}. \tag{3.19}$$

Finally, we have to take into account the lattice corrections due to the contribution δS. It will be useful to split them into two parts. The first one, denoted by δS_a, contains the terms of $\mathcal{L}_a$ in (2.3). These terms start at $\mathrm{O}(\epsilon^{n_a})$ (having taken into account ϵ^{-4} from the integration over space-time),

$$\delta S_a \sim \epsilon^{n_a}. \tag{3.20}$$

The second contribution, δS_{a^2}, contains only the a^2 term proportional to c_2. Therefore, it counts as

$$\delta S_{a^2} \sim \epsilon^{2n_a-4}. \tag{3.21}$$

After these preparations we can determine at which order the lattice spacing effects enter the PP and the AA correlator.

3.3.1 GSM regime

In the GSM regime we set $n_a = 4$ and find

$$\delta\langle P^a(x)P^a(0)\rangle \sim \mathrm{O}(\epsilon^4), \tag{3.22}$$

$$\delta\langle A^a_\mu(x)A^a_\mu(0)\rangle \sim \mathrm{O}(\epsilon^8). \tag{3.23}$$

The corrections due to the lattice spacing first affect both correlators at NNLO. Up to NLO the results obtained in continuum ChPT are the appropriate ones. This is quite remarkable and may explain why numerical data generated recently [22] could be fitted very well using the NLO continuum expressions. Note that this suppression to NNLO holds for the unimproved theory. The reason is that the terms linear in a are accompanied by at least one additional power of m or $\partial_\mu\xi$, and are therefore of higher order.

JHEP03(2009)006

3.3.2 GSM* regime

Here we have $n_a = 3$ and obtain

$$\delta\langle P^a(x)P^a(0)\rangle \sim \mathrm{O}(\epsilon^2)\,, \tag{3.24}$$

$$\delta\langle A^a_\mu(x)A^a_\mu(0)\rangle \sim \mathrm{O}(\epsilon^6)\,, \tag{3.25}$$

hence the corrections enter at NLO. Interestingly, the dominant term here comes only from the correction δS_{a^2}. The other corrections from the $\mathrm{O}(a)$ contributions in the currents, densities and δS_a start at ϵ^3 and ϵ^7, respectively. Therefore, they are of higher order in the epsilon expansion, even though they are still lower than the NNLO contributions, which start at ϵ^4 and ϵ^8, respectively.

Notice that in the GSM and GSM* regimes the leading order partition function is like the continuum one given in eq. (3.5). In particular, the exact zero-mode integrals are computed with respect to the same Boltzmann factor as in continuum ChPT.

3.3.3 Aoki regime

The modifications in the Aoki regime are more pronounced than in the previously discussed regimes. Here, cut-off effects show up already at LO. Even worse, the corrections can no longer be linearly added to the continuum result. The reason is the correction δS_{a^2}, which gives a zero-mode contribution of order ϵ^0. Hence, it is no longer justified to expand completely the exponential $\exp(-S_{a^2}) \approx 1 - S_{a^2}$. The zero-mode contribution of order ϵ^0 has to be included in the leading order Boltzmann factor. That is, the partition function becomes

$$Z_{\mathrm{Aoki}} = \int_{\mathrm{SU}(2)} [dU_0] \int [d\xi] \exp\left\{ \frac{1}{2}\int_V d^4x \mathrm{Tr}(\partial_\mu\xi\partial_\mu\xi) + \frac{m\Sigma V}{2}\mathrm{Tr}(U_0 + U_0^\dagger) \right. \tag{3.26}$$

$$\left. - \frac{c_2 F^2 a^2 V}{16}(\mathrm{Tr}(U_0 + U_0^\dagger))^2 \right\}.$$

This modification affects all constant integrals and probably leads to non-trivial changes of the continuum results. Note that the other $\mathrm{O}(a)$ corrections (from δO and δS_a) are of order ϵ^2 and show up at NLO only.

3.4 Comment on O(a) improvement

The results in the previous section are valid for unimproved Wilson fermions. It is natural to ask how (non-perturbative) $\mathrm{O}(a)$–improvement changes these results.

If the theory is non-perturbatively improved the corrections δO and δS_a are absent, and modifications are caused by δS_{a^2} only. We have seen that this term is the dominant correction and the others are subleading. Consequently, the epsilon expansion is essentially unaltered for the improved theory, since only subleading terms vanish.

4 Leading correction in the GSM* regime

We already mentioned in the introduction that the epsilon expansion is advantageous for the determination of F and Σ, since the Gasser-Leutwyler coefficients first enter the ChPT

JHEP03(2009)006

formulae at NNLO. The same is true for WChPT in the GSM regime, where the additional lattice spacing contributions enter at NNLO too. In other words, working through NLO the results for the GSM regime are the same as those in continuum ChPT.

The first non-trivial modification of the continuum NLO results appears in the GSM* regime, and in this section we compute the leading correction to the PP and AA correlator; the results for some other correlators are given in appendix C. This correction is caused by the constant term of the δS_{a^2} contribution,

$$\delta\langle O_1(x)O_2(y)\rangle\Big|_{\text{leading}} = -\langle O^{\text{LO}}_{1,\text{ct}}(x)O^{\text{LO}}_{2,\text{ct}}(y)\delta S_{a^2}\rangle + \langle O^{\text{LO}}_{1,\text{ct}}(x)O^{\text{LO}}_{2,\text{ct}}(y)\rangle\langle\delta S_{a^2}\rangle\,, \quad (4.1)$$

where

$$\delta S_{a^2} = \frac{\rho}{16}(\text{Tr}(U_0+U_0))^2. \quad (4.2)$$

The superscript "LO" refers to leading order in the ϵ-expansion and we have introduced the dimensionless quantity

$$\rho = F^2 c_2 a^2 V. \quad (4.3)$$

Notice that if $\langle O^{\text{LO}}_{1,\text{ct}}(x)O^{\text{LO}}_{2,\text{ct}}(y)\delta S_{a^2}\rangle = \langle O^{\text{LO}}_{1,\text{ct}}(x)O^{\text{LO}}_{2,\text{ct}}(y)\rangle\langle\delta S_{a^2}\rangle$, i.e for disconnected insertions, the leading correction in eq. (4.1) vanishes. This happens for instance for left handed (V-A) current correlators [46], and more general for correlators which do not get zero-mode contributions at leading order.

Since chiral symmetry is explicitly broken in Lattice QCD with Wilson fermions, a natural definition for the topological charge does not exist at non-zero lattice spacing. Moreover, a WChPT analysis of topology and its cut-off effects has not been done so far. For this reason we will only give results for observables where the sum over all topological sectors has been performed, even though the projection onto topological sectors via a Fourier transform [6] seems to be possible.

4.1 Preliminaries

Calculations of mesonic 2-point functions in the ϵ-regime have been pioneered in ref. [45]. The integration over the non-constant modes $\xi(x)$ is done perturbatively as in ordinary chiral perturbation theory in the p-regime. We summarize the corresponding propagators and other useful properties in appendix A.

The integral over the constant mode U_0 has to be done exactly. In our particular case with $N_f = 2$ we encounter integrals of the type

$$\langle g(U_0)\rangle = \frac{1}{Z_0}\int_{\text{SU}(2)}[dU_0]\, g(U_0)\, e^{\frac{\mu}{2}\text{Tr}(U_0+U_0^\dagger)}\,, \quad (4.4)$$

where Z_0 is the continuum partition function associated to the zero modes,

$$Z_0 = \int_{\text{SU}(2)}[dU_0] e^{\frac{\mu}{2}\text{Tr}(U_0+U_0^\dagger)}\,, \quad (4.5)$$

JHEP03(2009)006

and μ denotes the standard combination

$$\mu = m\Sigma V\,. \tag{4.6}$$

Quite generally, the integral (4.4) leads, at least for the types of g we are considering, to expressions involving modified Bessel functions $I_n(z)$ with integer index n. They satisfy numerous recursion relations [47], and all integrals can be expressed in terms of two Bessel functions, which we choose to be I_2 and I_1. In appendix B we collect various integrals that one encounters in calculating the PP and AA correlator in the GSM* regime.

As an example let us consider the expectation value of the quantity δS_{a^2}, defined in eq. (4.2), that is part of the correction in (4.1). By using the integrals given in the appendix we obtain

$$\langle \delta S_{a^2} \rangle = \rho \left(1 - \frac{3}{2\mu} \frac{I_2(2\mu)}{I_1(2\mu)} \right) . \tag{4.7}$$

4.2 The PP correlator

For the PP correlator we introduce the definition

$$\langle P^a(x) P^b(y) \rangle = \delta^{ab} C_{PP}(x-y)\,, \tag{4.8}$$

which takes into account translation invariance and the trivial dependence on the flavor indices. In the GSM* regime, $C_{PP}(x-y)$ can be written through NLO as the sum of the continuum correlator and a correction proportional to a^2,

$$C_{PP}(x-y) = C_{PP,\mathrm{ct}}(x-y) + C_{PP,a^2}(x-y)\,. \tag{4.9}$$

The continuum correlator for generic N_f at NLO (which corresponds to $O(\epsilon^2)$) is given by [45] (see also [48])

$$C_{PP,\mathrm{ct}}(x-y) = C_P + \alpha_P \bar{G}(x-y), \tag{4.10}$$

where $\bar{G}(x-y)$ is the finite-volume massless scalar propagator defined in eq. (A.1) and

$$C_P = -\frac{\Sigma_{\mathrm{eff}}^2}{8(N_f^2-1)} \left[\langle \mathrm{Tr}[(U_0 - U_0^\dagger)^2] \rangle_{\mathrm{eff}} - \frac{1}{N_f} \langle [\mathrm{Tr}(U_0 - U_0^\dagger)]^2 \rangle_{\mathrm{eff}} \right] , \tag{4.11}$$

$$\begin{aligned} \alpha_P = \frac{\Sigma^2}{4F^2(N_f^2-1)} \Bigg[& 2N_f^2 - 4 - \frac{2}{N_f} \langle \mathrm{Tr}(U_0^2) + \mathrm{Tr}(U_0^{\dagger 2}) \rangle \\ & + \frac{2}{N_f^2} \langle \mathrm{Tr}(U_0)\mathrm{Tr}(U_0^\dagger) \rangle + \left(\frac{N_f^2+1}{N_f^2} \right) \langle (\mathrm{Tr}U_0)^2 + (\mathrm{Tr}U_0^\dagger)^2 \rangle \Bigg] . \end{aligned} \tag{4.12}$$

The expectation values with the subscript "eff" are defined like in eq. (4.4) with μ replaced by

$$\mu_{\mathrm{eff}} = m\Sigma_{\mathrm{eff}} V, \tag{4.13}$$

where Σ_{eff} is the quark condensate at one loop [45]

$$\Sigma_{\mathrm{eff}} = \Sigma \left(1 + \frac{N_f^2-1}{N_f} \frac{1}{F^2} \frac{\beta_1}{\sqrt{V}} \right) . \tag{4.14}$$

JHEP03(2009)006

β_1 is a so-called *shape factor* and is defined in eq. (A.5).

For the particular case $N_f = 2$, after the explicit computation of the zero-mode integrals according to appendix B, one gets

$$C_P = \frac{\Sigma_{\rm eff}^2}{2\mu_{\rm eff}} \frac{I_2(2\mu_{\rm eff})}{I_1(2\mu_{\rm eff})}, \tag{4.15}$$

$$\alpha_P = \frac{\Sigma^2}{2F^2}\left[2 - \frac{1}{\mu}\frac{I_2(2\mu)}{I_1(2\mu)}\right]. \tag{4.16}$$

For the leading lattice correction to the continuum result, as given in eq. (4.1), we find the $O(\epsilon^2)$ contribution

$$C_{PP,a^2} = \rho\frac{\Sigma^2}{2}\Delta_{PP}, \tag{4.17}$$

with

$$\Delta_{PP} = \frac{5\mu I_1^2(2\mu) - 10 I_1(2\mu) I_2(2\mu) - 3\mu I_2^2(2\mu)}{2\mu^3 I_1^2(2\mu)}. \tag{4.18}$$

Interestingly, the correction Δ_{PP} is finite in the limit $\mu \to 0$, as is easily checked using the leading order Taylor expansions for the Bessel functions [47], $I_1(2\mu) \sim \mu$ and $I_2(2\mu) \sim \mu^2/2$. We are not aware of a rigorous argument that Δ_{PP} has to be regular at vanishing μ, since this correction ceases to be valid for small enough quark mass where one enters the Aoki regime. A singularity at $\mu = 0$ would have been a clear signal for this breakdown of our calculation, however, this signal is not present in the result, at least not at the order in the chiral expansion we are working here.

For the matching with numerical results obtained in lattice simulations we are interested in the correlation function integrated over the spatial components,

$$C_{PP}(t) = \int d^3\vec{x}\, C_{PP}(x-y)\Big|_{y=0} = C_{PP,\rm ct}(t) + \frac{L^3\Sigma^2}{2}\rho\Delta_{PP}\,, \tag{4.19}$$

where

$$C_{PP,\rm ct}(t) = \frac{L^3}{2}\frac{\Sigma_{\rm eff}^2}{\mu_{\rm eff}}\frac{I_2(2\mu_{\rm eff})}{I_1(2\mu_{\rm eff})} + \frac{T\Sigma^2}{2F^2}h_1(t/T)\left[2 - \frac{1}{\mu}\frac{I_2(2\mu)}{I_1(2\mu)}\right]. \tag{4.20}$$

The time dependence is given by the parabolic function h_1 defined in eq. (A.9).

4.3 The AA correlator

The AA correlator is computed along the same lines. For simplicity we consider the time-component correlator and we define

$$\langle A_0^a(x) A_0^b(y)\rangle = \delta^{ab} C_{AA}(x-y)\,. \tag{4.21}$$

Similarly to the PP correlator we split $C_{\rm AA}$ at NLO into a continuum part and a correction proportional to the lattice spacing,

$$C_{AA}(x-y) = C_{AA,\rm ct}(x-y) + C_{AA,a^2}(x-y)\,. \tag{4.22}$$

The continuum contribution at $O(\epsilon^6)$ for $x \neq y$ and generic N_f has been calculated before [45] (see also [49]) and is given by

$$C_{AA,\mathrm{ct}}(x-y) = \alpha_A \partial_{x_0}\partial_{y_0}\bar{G}(x-y) + \beta_A K_{00}(x-y) + \gamma_A \partial_{x_0}\partial_{y_0} H(x-y), \tag{4.23}$$

where the following short hand notation has been introduced:

$$\alpha_A = \frac{F^2}{2}\langle \mathcal{J}_0\rangle_{\mathrm{eff}} + \frac{N_f}{2}\frac{\beta_1}{\sqrt{V}}\langle \mathcal{J}_0\rangle\,, \tag{4.24}$$

$$\beta_A = \frac{N_f}{2}\left(2 - \langle \mathcal{J}_0\rangle\right)\,, \tag{4.25}$$

$$\gamma_A = \langle \mathrm{Tr}(U_0 + U_0^\dagger)\rangle \frac{\mu}{N_f}. \tag{4.26}$$

The functions $K_{\mu\nu}$ and H are given in eqs. (A.7) and (A.8). Moreover, we have introduced the quantity

$$\mathcal{J}_0 = \frac{1}{N_f^2-1}\left[\mathrm{Tr}U_0\mathrm{Tr}U_0^\dagger + N_f^2 - 2\right]. \tag{4.27}$$

Like for the PP correlator, the subscript "eff" refers to the substitution $\mu \to \mu_{\mathrm{eff}}$ in the zero-mode integrals. For the particular case we are considering, $N_f = 2$, the results (4.24)–(4.26) reduce to

$$\alpha_A = F^2\left[1 - \frac{I_2(2\mu_{\mathrm{eff}})}{\mu_{\mathrm{eff}} I_1(2\mu_{\mathrm{eff}})}\right] + 2\frac{\beta_1}{\sqrt{V}}\left[1 - \frac{I_2(2\mu)}{\mu I_1(2\mu)}\right]\,, \tag{4.28}$$

$$\beta_A = \frac{2}{\mu}\frac{I_2(2\mu)}{I_1(2\mu)}\,, \tag{4.29}$$

$$\gamma_A = \frac{2\mu I_2(2\mu)}{I_1(2\mu)}. \tag{4.30}$$

In analogy to the PP correlator, the $O(a^2)$ contribution can be computed according to eq. (4.1), and we obtain

$$C_{AA,a^2}(x-y) = \frac{F^2}{2}\partial_{x_0}\partial_{y_0}\bar{G}(x-y)\rho\Delta_{AA}\,, \tag{4.31}$$

with

$$\Delta_{AA} = \frac{-5\mu I_1^2(2\mu) + 10 I_1(2\mu) I_2(2\mu) + 3\mu I_2(2\mu)^2}{\mu^3 I_1^2(2\mu)} = -2\Delta_{PP}\,. \tag{4.32}$$

Note that this correction affects only the coefficient α_A in eq. (4.28), which will be modified by the presence of lattice artifacts.

The O(a^2) correction is, up to a sign and a factor two, the same as the correction for the PP correlator. As far as we can see there is no deeper reason for this. It is simply a consequence of the fact that the zero-mode integrals for the leading order continuum PP and AA correlator are very similar, both lead to the same contribution involving the ratio $I_2(2\mu)/\mu I_1(2\mu)$.

JHEP03(2009)006

By integrating over the spatial coordinates and using the properties listed in appendix A, we obtain for $t \neq 0$

$$C_{AA}(t) = \int d^3\vec{x}\, C_{AA}(x-y)|_{y=0} = C_{AA,\mathrm{ct}}(t) - \frac{F^2}{2T}\rho\Delta_{AA}, \tag{4.33}$$

where the continuum result for $N_f = 2$ explicitly reads

$$\begin{aligned} C_{AA,\mathrm{ct}}(t) &= -\frac{1}{T}\alpha_A + \frac{T}{V}k_{00}\beta_A - \frac{T}{V}\gamma_A h_1\left(\frac{t}{T}\right) = \\ &= -\frac{F^2}{T}\left(1 - \frac{I_2(2\mu_{\mathrm{eff}})}{\mu_{\mathrm{eff}} I_1(2\mu_{\mathrm{eff}})}\right) - \frac{2\beta_1}{T\sqrt{V}}\left(1 - \frac{I_2(2\mu)}{\mu I_1(2\mu)}\right) + \\ &\quad + \frac{2T}{V}k_{00}\frac{I_2(2\mu)}{\mu I_1(2\mu)} - \frac{2T}{V}h_1(t/T)\frac{\mu I_2(2\mu)}{I_1(2\mu)}\,. \end{aligned} \tag{4.34}$$

Here k_{00} is another shape factor defined in the appendix, eq. (A.6).

4.4 The PCAC mass

The correlators in the previous section are given as functions of m, the shifted mass. This is the mass parameter in the chiral Lagrangian and a priori not an observable. Here we compute the PCAC mass, defined in (2.16), and use it in the next section to replace m with m_{PCAC}.

We have already calculated the denominator of (2.16), and the numerator can be done analogously. Let us define

$$\langle \partial_\mu A^a_\mu(x) P^b(y)\rangle = \delta^{ab} C_{\partial AP}(x-y)\,. \tag{4.35}$$

To leading order in the epsilon expansion we find the result

$$C_{\partial AP,\mathrm{ct}}(x-y) = \frac{\Sigma}{V}\frac{I_2(2\mu)}{I_1(2\mu)}\,. \tag{4.36}$$

Dividing this by the leading order result of $2C_{PP,\mathrm{ct}}$ in eq. (4.10) we obtain

$$m_{\mathrm{PCAC}} = \frac{\mu}{\Sigma V} = m\,. \tag{4.37}$$

This is just the result of continuum ChPT, where it is not surprising because the PCAC mass stems from the PCAC Ward identity. Note, however, that both numerator and denominator contain non-trivial Bessel functions which cancel in the ratio. This cancellation will no longer happen with the lattice spacing corrections included, since the PCAC relation no longer holds.

The leading correction to the numerator in the GSM* regime is given by (4.1) with $O_1 = \partial_\mu A^a(x)$ and $O_2 = P^a(y)$ (no sum over a). The computation is straightforward as the ones in the previous sections and we find

$$C_{\partial AP}(x-y) = \frac{\Sigma}{V}\frac{I_2(2\mu)}{I_1(2\mu)}\left[1 - \frac{3\rho}{2\mu^2}\left(2 - \frac{\mu I_1(2\mu)}{I_2(2\mu)} + \frac{\mu I_2(2\mu)}{I_1(2\mu)}\right)\right]. \tag{4.38}$$

Dividing by $2C_{PP}$ given in (4.9) we obtain the leading $O(a^2)$ corrections to the PCAC mass:

$$m_{\rm PCAC} = m\left[1+\rho\left(\frac{2}{\mu^2}-\frac{I_1(2\mu)}{\mu I_2(2\mu)}\right)\right]. \tag{4.39}$$

The key observation here is that the PCAC mass is equal to m, up to a correction of $\mathrm{O}(ma^2V)$, which is ϵ^2 higher in the epsilon expansion in the GSM* regime.

4.5 The correlators as a function of the PCAC mass

The final step we have to do is to replace m by $m_{\rm PCAC}$ in the correlators. We first invert result (4.39),

$$\mu = \tilde{\mu}\left[1-\rho\left(\frac{2}{\tilde{\mu}^2}-\frac{I_1(2\tilde{\mu})}{\tilde{\mu}I_2(2\tilde{\mu})}\right)\right], \tag{4.40}$$

where

$$\tilde{\mu} = m_{\rm PCAC}\Sigma V. \tag{4.41}$$

In the NLO contributions of the correlators we can simply replace $m = m_{\rm PCAC}$, $\mu = \tilde{\mu}$, since the corrections are higher than this order. In the LO term, however, we have to use the full expression (4.40), which gives rise to additional corrections proportional to ρ.

Eq. (4.40) has to be inserted into the Bessel functions $I_n(2\mu)$. Since the correction proportional to ρ is ϵ^2 higher in the epsilon expansion we can Taylor-expand,

$$I_n(2\mu) = I_n(2\tilde{\mu}) - 2\rho\tilde{\mu}I_n'(2\tilde{\mu})\left(\frac{2}{\tilde{\mu}^2}-\frac{I_1(2\tilde{\mu})}{\tilde{\mu}I_2(2\tilde{\mu})}\right)+\ldots \tag{4.42}$$

and drop the higher order terms. The final results for the correlators can be brought into the form

$$C_{PP}(t) = C_{PP,\rm ct}(t) + \frac{L^3\Sigma^2}{2}\rho\Delta_{a^2}, \tag{4.43}$$

$$C_{AA}(t) = C_{AA,\rm ct}(t) + \frac{F^2}{T}\rho\Delta_{a^2}, \tag{4.44}$$

where the continuum correlators are as in (4.20) and (4.34), but with the replacements $\mu \to \tilde{\mu}$ and $\mu_{\rm eff} \to \tilde{\mu}_{\rm eff}$, with

$$\tilde{\mu}_{\rm eff} = m_{\rm PCAC}\Sigma_{\rm eff}V. \tag{4.45}$$

The correction Δ_{a^2}, which depends on $\tilde{\mu}$, captures the lattice spacing artifacts and reads

$$\Delta_{a^2} = \frac{4\tilde{\mu}^2I_1^3(2\tilde{\mu}) - 11\tilde{\mu}I_1^2(2\tilde{\mu})I_2(2\tilde{\mu}) + 2(3-2\tilde{\mu}^2)I_1(2\tilde{\mu})I_2^2(2\tilde{\mu}) + 5\tilde{\mu}I_2^3(2\tilde{\mu})}{2\tilde{\mu}^3I_1^2(2\tilde{\mu})I_2(2\tilde{\mu})}. \tag{4.46}$$

Note that it is regular at $\tilde{\mu} = 0$.

Eqs. (4.43) and (4.44) are our final results for the GSM* regime. (In appendix C we also give the corresponding expression for the vector current correlator.) These results are remarkable and perhaps surprising in two ways: (i) The $\tilde{\mu}$ dependence of the $\mathrm{O}(a^2)$

JHEP03(2009)006

correction is identical for both correlation functions. (ii) Besides the continuum LECs F and Σ only one more unknown LEC enters these expression, the parameter c_2. The second feature is very advantageous in practice when our results are used to fit numerical lattice data.

A different question is the actual size of the $O(a^2)$ correction, which is directly proportional to c_2. In the next section we try to give at least a rough answer to this question.

5 Numerical tests

5.1 General considerations

For the pseudo scalar and axial vector correlators, the leading $O(a^2)$ correction in the GSM* regime is just a shift of the constant part. The question is how big this correction is in a typical ϵ-regime simulation. As a measure for the correction we study the ratio

$$R_{\mathrm{XX}} = \left| \frac{C_{\mathrm{XX}}(T/2) - C_{\mathrm{XX,ct}}(T/2)}{C_{\mathrm{XX,ct}}(T/2)} \right| , \tag{5.1}$$

i.e. the relative shift of the correlators at $T/2$. The main unknown here is the coefficient c_2. Even though it plays a decisive role in the phase diagram of the theory [32], it is difficult to obtain in numerical simulations. So far only the ETM collaboration has obtained an estimate from their simulations with a twisted mass term [26, 50]. The data for the pion mass splitting together with the LO ChPT prediction gives the rough estimate $-2c_2a^2 \approx (185\mathrm{MeV})^2$ at $a \approx 0.086\mathrm{fm}$, which translates into $|c_2| \approx (550\mathrm{MeV})^4$. The error, however, is fairly large because of the large statistical error in the determination of the neutral pion mass. In addition, this value for c_2 was obtained with the tree-level Symanzik improved gauge action and the standard Wilson fermion action, and any change in this setup can and probably will lead to a different value for c_2.[9] Nevertheless, for lack of a better estimate we use $|c_2| = (500\mathrm{MeV})^4$ in the following.

For the other parameters we use $F = 90\mathrm{MeV}$, $a = 0.08\mathrm{fm}$ and a hypercubic lattice with $N_T = N_L = 24$, which corresponds to a box size $L = 1.92\mathrm{fm}$. This implies $\rho \approx 0.75$. Even though this is slightly large we may still count this as $O(\epsilon^2)$ as it should in order to be in the GSM* regime.

Figure 1 shows R_{PP} and R_{AA} for $\tilde{\mu}$ values in the ϵ-regime. For $\tilde{\mu} = 1.0$ we find $R_{PP} = 2.8\%$ and it decreases to less than 1% for $\tilde{\mu}$ larger than 2. The correction is maximal (less than 5%) at vanishing $\tilde{\mu}$. However, for $\tilde{\mu} \sim \rho$ we enter the Aoki regime and our formulae are no longer valid. The values for R_{AA} are very similar. For instance, $R_{AA} = 2.1\%$ at $\tilde{\mu} = 1.0$.

Figure 1 also shows $\Delta_{a^2}(\tilde{\mu})$, which is, up to the factor ρ, the numerator in (5.1). It looks very similar to the ratios itself, since the denominator in (5.1) is of O(1) and varies only mildly for the $\tilde{\mu}$ values considered her. So the correction to the correlators is essentially $\Delta_{a^2}(\tilde{\mu})$, which happens to be of the order of 10^{-2}.

[9] An analysis [51] of quenched twisted mass lattice data led to a value $c_2 \approx (300\mathrm{MeV})^4$.

JHEP03(2009)006

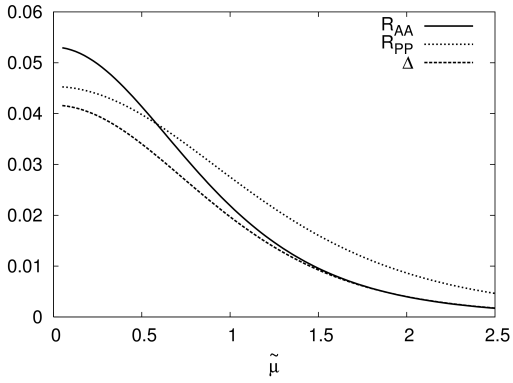

Figure 1. R_{PP} (dotted) and R_{AA} (solid) as a function of $\tilde{\mu}$. Both ratios are smaller than 3.5% for $\tilde{\mu} \geq 0.75$. The dashed curve represents $\Delta_{a^2}(\tilde{\mu})$.

The main conclusion we can draw from this exercise is that for our choice of parameters the $O(a^2)$ corrections to the correlators are at the few percent level, a comfortably small value.

Using a bigger box improves the epsilon expansion since the expansion parameter $1/(FL)^2$ is smaller. However, a bigger box also leads to larger ρ values and one easily enters the Aoki regime at moderately large volumes. For instance, with $N_L = 32$ and the other parameters unchanged we get $L = 2.4\,\text{fm}$ and $\rho \approx 2.4$, a value that is certainly not $O(\epsilon^2)$.[10]

5.2 Reanalysis of recent lattice data

In this section we investigate the impact of c_2 on the extraction of the continuum low energy constants F and Σ from lattice data. The data is taken from refs. [22, 52]. It is generated with $N_f = 2$ flavors of dynamical improved NHYP Wilson fermions [53] at a fairly small quark mass. From there, a reweighting procedure allows to access even smaller sea quark masses [23]. This procedure is exact and does not introduce systematic uncertainties but allows to compute correlators at very small quark masses at moderate cost. The lattice spacing is $a \approx 0.115\text{fm}$ from the measurement of the Sommer parameter r_0 taken to be 0.49fm [54]. We have two volumes available, one at $L = 16a \approx 1.84\text{fm}$ and a larger one with $L = 24a \approx 2.8\text{fm}$. The former serves mainly as a cross check whereas the latter has sufficient size for our NLO formulae to be applicable. Some parameters of the simulation are given in table 1.

The theoretical formulae for the pseudo scalar and axial vector correlator both have the form constant plus parabola. The coefficient c_2 only contributes to the constant term in both cases. The curvature itself is rather small at the parameter values simulated, in particular compared to the statistical uncertainties, see figure 2. Therefore, at a fixed mass,

[10] It may seem counterintuitive at first that a change in the volume may bring us into a different regime. However, increasing the volume requires that we need to decrease the mass in order to stay in the ϵ-regime with fixed $\tilde{\mu}$. Hence we have to decrease a as well in order to preserve the relative size between the mass and the lattice spacing terms.

JHEP03(2009)006

L/a	κ	am_{PCAC}	μ
24	0.128150	0.0019(4)	2.1
	0.128125	0.0024(3)	2.7
	0.128100	0.0030(3)	3.4
	0.128050	0.0044(3)	5.0
16	0.128100	0.0028(11)	0.7
	0.128050	0.0047(9)	1.1
	0.128000	0.0058(7)	1.4
	0.127900	0.0088(5)	2.1
	0.127800	0.0117(3)	2.9

Table 1. Parameters of the simulation. L/a is the extend of the box, κ the hopping parameters, the PCAC quark mass and an approximate values of $\mu = m\Sigma V$, where we use the central value of Σ.

each of the two correlators effectively is a constant from which it is difficult to constrain three parameters. As already discussed, the theory predicts a particular and relatively strong $\tilde{\mu}$ dependence of the term multiplied by c_2. This gives a handle on the extraction of this coefficient. Therefore we simultaneously fit the axial vector and pseudo scalar correlators for all available quark masses. From a fit to $t \in [6, 18]$ we get $\Sigma^{1/3} = 249(4)$MeV, $F = 88(3)$MeV and $c_2 = 0.02(8)\mathrm{GeV}^4$. The data, along with the theoretical curves can be found in figure 2. Here we used $Z_P^{\overline{\mathrm{MS}}}(2\mathrm{GeV}) = 0.90(2)$ and $Z_A = 0.99(2)$ from ref. [22]. The errors from the renormalization factors are not included in the uncertainties of the LECs. The value of c_2 is compatible with zero within errors and the one sigma band lies within the range of reasonable values for a low energy constant. Since the data points are highly correlated, we cannot give a good estimate for the quality of the fit; we find $\chi^2/\mathrm{dof} = 0.3(1)$ without the correlations taken into account. We also remark that the results are independent of the fit range once $t_{\mathrm{min}}/a > 4$. Another concern are the relatively large values of $\tilde{\mu}$. Therefore we repeated the analysis leaving the $\tilde{\mu} \approx 5$ data out. We get from the same fit range $\Sigma^{1/3} = 250(4)$MeV, $F = 87(3)$MeV and $c_2 = -0.01(8)\mathrm{GeV}^4$. The differences to the previous values are well within the statistical uncertainties. This is encouraging. Even with the additional constant the errors of the continuum LECs are reasonably small.

Is the value we find for c_2 large or not? To gauge the impact of this term, we repeat the fit by setting $c_2 = 0$. The results are virtually unchanged within errors: $\Sigma^{1/3} = 249(4)$MeV, $F = 88(3)$MeV. This is very good news. The cut-off effects are so small that they do not impact the extraction of the low energy constants beyond the level of the statistical uncertainties.

As a cross check we repeated this analysis on the smaller volume, at the same lattice spacing and $L/a = 16$. We obtain $\Sigma^{1/3} = 257(4)$MeV, $F = 83(2)$MeV and $c_2 = 0.06(14)\mathrm{GeV}^4$. However, the (uncorrelated) $\chi^2/\mathrm{dof} = 1.3$ might indicate that the NLO formulae are no longer applicable. These results agree with the findings of ref. [22].

JHEP03(2009)006

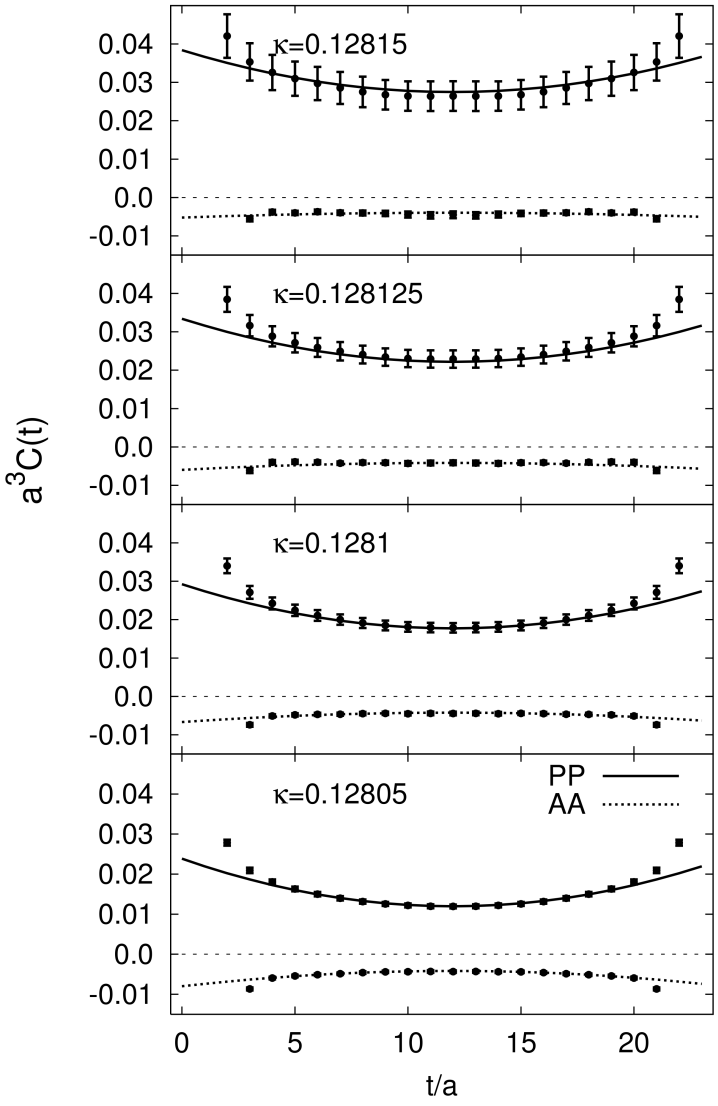

Figure 2. Fit of the WChPT predictions to lattice data. All data points within the fit range of $t/a \in [6, 18]$ for the four sea quark masses are included in the combined fit. The axial vector correlator is multiplied by a factor 50 for better visibility.

6 Conclusions

We have shown that the corrections due to the explicit chiral symmetry breaking of Wilson fermions are highly suppressed. For typical quark masses these corrections enter at either NNLO (GSM regime) or at NLO (GSM* regime). The reason for this suppression can be traced back to the fact that the lattice spacing corrections in the chiral effective action and the effective operators are either quadratic in a or they come with an additional power of either m or p^2. There is no explicit term with a single power of a only, since such a term

JHEP03(2009)006

solely contributes to the additive mass renormalization which is absorbed in the quark mass. Hence, the lattice spacing corrections are suppressed in the chiral expansion, similar to the terms in the Gasser-Leutwyler Lagrangian $\mathcal{L}_4$.

In the Aoki regime the modifications are more substantial, affecting the correlators already at LO. The main complication in this regime are the zero mode integrals, which are no longer the known Bessel functions.

We tested our formulae against recent lattice data. We found that the additional terms which come from the broken chiral symmetry have very little impact on the extracted values of F and Σ whereas the low-energy constant associated with the breaking is hard to determine precisely.

Our results derived here can be generalized in various ways, for example to the case with a twisted mass term or to an arbitrary number of flavors. The details of the calculation will change, but our various power countings can be carried over with almost no modification. Perhaps most interesting from a practical point of view is an extension along the lines of ref. [55], where one considers a mixed setup with some quarks in the ϵ-regime and some others in the p-regime.

However, the main conclusion one can draw is that the effects due to explicit chiral symmetry breaking of Wilson fermions in the ϵ-regime are less severe than anticipated before. In view of the results of ref. [22] and the ones presented here, simulations with Wilson fermions seem to be a viable alternative to the daunting task of dynamical simulations with chiral fermions.

Note added. After this paper was completed we received a paper by A. Shindler which also deals with Wilson fermions in the ϵ-regime and comes to essentially the same conclusions [56]. Our result for the $O(a^2)$ correction to the PP correlator in the GSM* regime agrees with the one in [56] (the AA correlator has not been computed in that reference).

Acknowledgments

We would like to thank A. Hasenfratz and P. Hernández for fruitful discussions and A. Hasenfratz for reading the manuscript.

S.N. is supported by Marie Curie Fellowship MEIF-CT-2006-025673, and thanks the Physics Institute of the Humboldt University (Berlin) for hospitality during the preparation of this work.

This work is partially supported by EC Sixth Framework Program under the contract MRTN-CT-2006-035482 (FLAVIAnet), by the Deutsche Forschungsgemeinschaft (SFB/TR 09) and the Ministerio de Ciencia e Innovación under Grant No. FPA2007-60323 and by CPAN (Grant No. CSD2007-00042).

A Some results for the epsilon regime

In this appendix we summarize formulae which are relevant for the computation of correlation functions in the ϵ-regime of chiral perturbation theory.

Starting from the leading order continuum chiral Lagrangian of eq. (2.1) and by introducing the parametrization of eq. (3.2), we can read off the finite-volume scalar propagator for the nonzero modes:

$$\bar{G}(x) = \frac{1}{V} \sum_{p \neq 0} \frac{e^{ipx}}{p^2}, \tag{A.1}$$

with

$$p = 2\pi \left(\frac{n_0}{T}, \frac{\vec{n}}{L} \right).$$

The propagator $\bar{G}(x)$ satisfies the following properties:

$$\int_V d^4x \, \bar{G}(x) = 0\,, \tag{A.2}$$

$$\partial_\mu \bar{G}(0) = 0\,, \tag{A.3}$$

$$\Box \bar{G}(x) = -\delta(x) + \frac{1}{V}. \tag{A.4}$$

UV divergencies, if present, are treated in dimensional regularization.
We define [45, 57]

$$\bar{G}(0) \equiv -\frac{\beta_1}{\sqrt{V}}\,, \tag{A.5}$$

$$T \frac{d}{dT} \bar{G}(0) \equiv \frac{T^2 k_{00}}{V}, \tag{A.6}$$

where β_1 and k_{00} are finite dimensionless *shape coefficients* which depend on the geometry of the box. They can be evaluated numerically: for instance, for a symmetric box with $L = T$ one has $\beta_1 = 0.140461$ and $k_{00} = \beta_1/2$ (see also [46]).

In order to obtain time correlators one has to perform integrals over the spatial components of given functions of the propagators $\bar{G}(x)$. In particular we define [45, 57] [11]

$$\begin{aligned} K_{\mu\nu}(x-y) &= \bar{G}(x-y)\partial_{x_\mu}\partial_{y_\nu}\bar{G}(x-y) - \partial_{x_\mu}\bar{G}(x-y)\partial_{y_\nu}\bar{G}(x-y) + \\ &+ \partial_{x_\mu}\partial_{y_\nu} H(x-y), \end{aligned} \tag{A.7}$$

$$H(x-y) = -\frac{1}{V}\int_V d^4z \bar{G}(x-z)\bar{G}(z-y). \tag{A.8}$$

The integrals that we need for this work are ($x_0 = t$):

$$\int d^3\vec{x}\, \bar{G}(x-y)|_{y=0} = T h_1\left(\frac{t}{T}\right) = \frac{T}{2}\left[\left(\left|\frac{t}{T}\right| - \frac{1}{2}\right)^2 - \frac{1}{12}\right], \tag{A.9}$$

$$\int d^3\vec{x}\, K_{00}(x-y)|_{y=0} = \frac{T}{V} k_{00}, \tag{A.10}$$

$$\partial_{x_0}\partial_{y_0} \int d^3\vec{x}\, H(x-y)|_{y=0} = -\frac{T}{V} h_1\left(\frac{t}{T}\right). \tag{A.11}$$

[11] In the original definition of [45, 57], $K_{\mu\nu}(x-y)$ contains also contact terms, which we do not consider in our computation since we are interested in the correlators for $x \neq y$.

Finally, we recall the SU(N_f) completeness relations which are used for the computation of correlation functions. Given the SU(N_f) generators T^a, with $a = 1, \ldots, N_f^2 - 1$ and the convention

$$\mathrm{Tr}[T^a T^b] = \frac{1}{2}\delta^{ab},$$

one obtains

$$\mathrm{Tr}(T^a A T^a B) = -\frac{1}{2N_f}\mathrm{Tr}(AB) + \frac{1}{2}\mathrm{Tr}(A)\mathrm{Tr}(B), \tag{A.12}$$

$$\mathrm{Tr}(T^a A)\mathrm{Tr}(T^a B) = -\frac{1}{2N_f}\mathrm{Tr}(A)\mathrm{Tr}(B) + \frac{1}{2}\mathrm{Tr}(AB). \tag{A.13}$$

B SU(2) integrals

In the case $N_f = 2$, the partition function related to the zero-mode integrals in eq. (4.5) is given by

$$Z_0 = \int_{\mathrm{SU}(2)} [dU_0] e^{\frac{\mu}{2}\mathrm{Tr}(U_0 + U_0^\dagger)} = \frac{I_1(2\mu)}{\mu}\,, \tag{B.1}$$

where I_n is the modified Bessel function of the first kind. The normalization

$$\int_{\mathrm{SU}(2)} [dU_0] = 1 \tag{B.2}$$

has been adopted. Expectation values of arbitrary integer powers of $\mathrm{Tr}(U_0)$ can be obtained by computing derivatives of Z_0. In particular, for this work we need

$$\langle \mathrm{Tr}U_0 \rangle = \frac{1}{Z_0}\frac{\partial Z_0}{\partial \mu} = 2\frac{I_2(2\mu)}{I_1(2\mu)}, \tag{B.3}$$

$$\langle (\mathrm{Tr}U_0)^2 \rangle = \frac{1}{Z_0}\frac{\partial^2 Z_0}{\partial \mu^2} = 4 - \frac{6}{\mu}\frac{I_2(2\mu)}{I_1(2\mu)}, \tag{B.4}$$

$$\langle (\mathrm{Tr}U_0)^3 \rangle = \frac{1}{Z_0}\frac{\partial^3 Z_0}{\partial \mu^3} = -\frac{12}{\mu} + \frac{8(3+\mu^2)I_2(2\mu)}{\mu^2 I_1(2\mu)}, \tag{B.5}$$

$$\langle (\mathrm{Tr}U_0)^4 \rangle = \frac{1}{Z_0}\frac{\partial^4 Z_0}{\partial \mu^4} = 16 + \frac{60}{\mu^2} - \frac{24(5+2\mu^2)I_2(2\mu)}{\mu^3 I_1(2\mu)}. \tag{B.6}$$

Other integrals needed in this work can be related to the previous ones, for instance:

$$\langle \mathrm{Tr}U_0^2 \rangle = 2 - \frac{3}{\mu}\langle \mathrm{Tr}U_0 \rangle = 2 - \frac{6}{\mu}\frac{I_2(2\mu)}{I_1(2\mu)}\,, \tag{B.7}$$

$$\begin{aligned}\langle \mathrm{Tr}U_0^2\,(\mathrm{Tr}U_0)^2 \rangle &= -\frac{6}{\mu^3}\langle \mathrm{Tr}U_0 \rangle + 2\left(1 + \frac{3}{\mu^2}\right)\langle (\mathrm{Tr}U_0)^2 \rangle - \frac{3}{\mu}\langle (\mathrm{Tr}U_0)^3 \rangle \\ &= \frac{4(15+2\mu^2)}{\mu^2} - \frac{12(10+3\mu^2)I_2(2\mu)}{\mu^3 I_1(2\mu)}.\end{aligned} \tag{B.8}$$

C Other correlators

Here we summarize the GSM* results for some other correlators. We start with the correlation function of the time component of two vector currents,

$$\langle V_0^a(x)V_0^b(y)\rangle \;=\; \delta^{ab}C_{VV}(x-y)\,, \tag{C.1}$$

which we again split into a continuum part and a correction proportional to the lattice spacing,

$$C_{VV}(x-y) \;=\; C_{VV,\mathrm{ct}}(x-y) + C_{VV,a^2}(x-y)\,. \tag{C.2}$$

In our notation the leading order vector current in the chiral effective theory reads

$$V^a_{\mu,\mathrm{ct}} \;=\; -i\frac{F^2}{2}\mathrm{Tr}\left(T^a(U^\dagger\partial_\mu U + U\partial_\mu U^\dagger)\right)\,. \tag{C.3}$$

The continuum contribution at $O(\epsilon^6)$ for generic N_f has been calculated before by Hansen [45] (see also [49]). After integrating over the spatial coordinates one gets

$$C^{ab}_{VV}(t) = \delta^{ab}\left[-\frac{1}{T}\alpha_V + \frac{T}{V}k_{00}\beta_V\right], \tag{C.4}$$

with

$$\alpha_V \;=\; \frac{F^2}{2}(2-\langle\mathcal{J}_0\rangle_{\mathrm{eff}}) + \frac{N_f}{2}\frac{\beta_1}{\sqrt{V}}(2-\langle\mathcal{J}_0\rangle), \tag{C.5}$$

$$\beta_V \;=\; \frac{N_f}{2}\langle\mathcal{J}_0\rangle. \tag{C.6}$$

The function $\mathcal{J}_0$ has been defined in eq. 4.27. In particular, for $N_f = 2$ the result explicitly reads

$$C^{ab}_{VV}(t) = -\frac{F^2}{T}\left(\frac{I_2(2\mu_{\mathrm{eff}})}{\mu_{\mathrm{eff}}I_1(2\mu_{\mathrm{eff}})}\right) - \frac{2\beta_1}{T\sqrt{V}}\left(\frac{I_2(2\mu)}{\mu I_1(2\mu)}\right) + \frac{2T}{V}k_{00}\left(1-\frac{1}{\mu}\frac{I_2(2\mu)}{I_1(2\mu)}\right). \tag{C.7}$$

The $\mathrm{O}(a^2)$ correction in terms of the PCAC mass is given by

$$C_{VV,a^2}(t) \;=\; -\frac{F^2}{T}\rho\Delta_{a^2}\,, \tag{C.8}$$

where Δ_{a^2} is defined in eq. (4.46). Comparing this with the result for the AA correlator in (4.44) we observe that the lattice spacing corrections in these two correlators are, up to a sign, identical.

With both the AA and the VV correlator at hand we can trivially obtain the correlation functions of right- and left-handed currents. For example, with $L^a_\mu = [V^a_\mu - A^a_\mu]/2$ we find

$$C_{LL}(t) \;=\; \frac{1}{4}\Big(C_{VV}(t) + C_{AA}(t)\Big)\,, \tag{C.9}$$

and the $\mathrm{O}(a^2)$ corrections cancel in the sum on the right hand side, i.e.

$$C_{LL,a^2}(t) \;=\; 0 \tag{C.10}$$

while the continuum part is given by [45, 46]

$$C_{LL,ct}(t) = \frac{1}{4}\left[-\frac{F^2}{T} - \frac{N_f}{T}\frac{\beta_1}{\sqrt{V}} + N_f\frac{T}{V}k_{00} - \frac{T}{V}\langle \mathrm{Tr}(U_0 + U_0^\dagger)\rangle \frac{\tilde{\mu}}{N_f} h_1\left(\frac{t}{T}\right)\right]$$
$$= \frac{1}{2}\left[-\frac{F^2}{2T} - \frac{1}{T}\frac{\beta_1}{\sqrt{V}} + \frac{T}{V}k_{00} - \frac{T}{V}\frac{\tilde{\mu} I_2(2\tilde{\mu})}{I_1(2\tilde{\mu})} h_1\left(\frac{t}{T}\right)\right]. \qquad \text{(C.11)}$$

The same result can be obtained by a direct calculation of the correlator, of course.

Finally, the scalar correlator

$$\langle S^a(x) S^b(y)\rangle = \delta^{ab} C_{SS}(x-y) \qquad \text{(C.12)}$$

vanishes identically in the chiral effective theory for $N_f = 2$, as one can check either by explicit calculation or by using G-parity.

References

[1] J. Gasser and H. Leutwyler, *Light quarks at low temperatures*, *Phys. Lett.* **B 184** (1987) 83 [SPIRES].

[2] J. Gasser and H. Leutwyler, *Thermodynamics of chiral symmetry*, *Phys. Lett.* **B 188** (1987) 477 [SPIRES].

[3] J. Gasser and H. Leutwyler, *Chiral perturbation theory to one loop*, *Ann. Phys.* **158** (1984) 142 [SPIRES].

[4] J. Gasser and H. Leutwyler, *Chiral perturbation theory: expansions in the mass of the strange quark*, *Nucl. Phys.* **B 250** (1985) 465 [SPIRES].

[5] S. Necco, *Determining QCD low-energy couplings from lattice simulations*, PoS(LATTICE 2007)021 [arXiv:0710.2444].

[6] H. Leutwyler and A.V. Smilga, *Spectrum of Dirac operator and role of winding number in QCD*, *Phys. Rev.* **D 46** (1992) 5607 [SPIRES].

[7] H. Neuberger, *Exactly massless quarks on the lattice*, *Phys. Lett.* **B 417** (1998) 141 [hep-lat/9707022] [SPIRES].

[8] D.B. Kaplan, *A Method for simulating chiral fermions on the lattice*, *Phys. Lett.* **B 288** (1992) 342 [hep-lat/9206013] [SPIRES].

[9] Y. Shamir, *Chiral fermions from lattice boundaries*, *Nucl. Phys.* **B 406** (1993) 90 [hep-lat/9303005] [SPIRES].

[10] V. Furman and Y. Shamir, *Axial symmetries in lattice QCD with Kaplan fermions*, *Nucl. Phys.* **B 439** (1995) 54 [hep-lat/9405004] [SPIRES].

[11] P. Hernández, K. Jansen and L. Lellouch, *Finite-size scaling of the quark condensate in quenched lattice QCD*, *Phys. Lett.* **B 469** (1999) 198 [hep-lat/9907022] [SPIRES].

[12] MILC collaboration, T.A. DeGrand, *Another determination of the quark condensate from an overlap action*, *Phys. Rev.* **D64** (2001) 117501 [hep-lat/0107014] [SPIRES].

[13] P. Hasenfratz, S. Hauswirth, T. Jorg, F. Niedermayer and K. Holland, *Testing the fixed-point QCD action and the construction of chiral currents*, *Nucl. Phys.* **B 643** (2002) 280 [hep-lat/0205010] [SPIRES].

JHEP03(2009)006

[14] W. Bietenholz, T. Chiarappa, K. Jansen, K.I. Nagai and S. Shcheredin, *Axial correlation functions in the ϵ-regime: a numerical study with overlap fermions*, *JHEP* **02** (2004) 023 [hep-lat/0311012] [SPIRES].

[15] L. Giusti, P. Hernández, M. Laine, P. Weisz and H. Wittig, *Low-energy couplings of QCD from current correlators near the chiral limit*, *JHEP* **04** (2004) 013 [hep-lat/0402002] [SPIRES].

[16] H. Fukaya, S. Hashimoto and K. Ogawa, *Low-lying mode contribution to the quenched meson correlators in the ϵ-regime*, *Prog. Theor. Phys.* **114** (2005) 451 [hep-lat/0504018] [SPIRES].

[17] W. Bietenholz and S. Shcheredin, *Overlap hypercube fermions in QCD simulations near the chiral limit*, *Nucl. Phys.* **B 754** (2006) 17 [hep-lat/0605013] [SPIRES].

[18] L. Giusti and S. Necco, *Spontaneous chiral symmetry breaking in QCD: a finite-size scaling study on the lattice*, *JHEP* **04** (2007) 090 [hep-lat/0702013] [SPIRES].

[19] L. Giusti et. al., *Testing chiral effective theory with quenched lattice QCD*, *JHEP* **05** (2008) 024 [arXiv:0803.2772] [SPIRES].

[20] S. Schaefer, *Algorithms for dynamical overlap fermions*, PoS(LAT2006)020.

[21] JLQCD collaboration, H. Fukaya et. al., *Lattice study of meson correlators in the ϵ-regime of two-flavor QCD*, *Phys. Rev.* **D77** (2008) 074503 [arXiv:0711.4965] [SPIRES].

[22] A. Hasenfratz, R. Hoffmann and S. Schaefer, *Low energy chiral constants from ϵ-regime simulations with improved Wilson fermions*, *Phys. Rev.* **D78** (2008) 054511 [arXiv:0806.4586] [SPIRES].

[23] A. Hasenfratz, R. Hoffmann and S. Schaefer, *Reweighting towards the chiral limit*, *Phys. Rev.* **D 78** (2008) 014515 [arXiv:0805.2369] [SPIRES].

[24] K. Jansen et al., *Exploring the epsilon regime with twisted mass fermions*, PoS(LATTICE 2007)084 [arXiv:0711.1871].

[25] K. Jansen, A. Nube and A. Shindler, *Wilson twisted mass fermions in the ϵ-regime*, arXiv:0810.0300 [SPIRES].

[26] C. Urbach, *Lattice QCD with two light Wilson quarks and maximally twisted mass*, PoS(LATTICE 2007)022 [arXiv:0710.1517].

[27] Alpha collaboration, R. Frezzotti, P.A. Grassi, S. Sint and P. Weisz, *Lattice QCD with a chirally twisted mass term*, *JHEP* **08** (2001) 058 [hep-lat/0101001] [SPIRES].

[28] ALPHA collaboration, R. Frezzotti, S. Sint and P. Weisz, *$O(a)$ improved twisted mass lattice QCD*, *JHEP* **07** (2001) 048 [hep-lat/0104014] [SPIRES].

[29] R. Frezzotti and G.C. Rossi, *Chirally improving Wilson fermions. I: $O(a)$ improvement*, *JHEP* **08** (2004) 007 [hep-lat/0306014] [SPIRES].

[30] S. Aoki and O. Bär, *Twisted-mass QCD, $O(a)$ improvement and Wilson chiral perturbation theory*, *Phys. Rev.* **D 70** (2004) 116011 [hep-lat/0409006] [SPIRES].

[31] S. Aoki and O. Bär, *Automatic $O(a)$ improvement for twisted-mass QCD in the presence of spontaneous symmetry breaking*, *Phys. Rev.* **D74** (2006) 034511 [hep-lat/0604018] [SPIRES].

[32] S.R. Sharpe and J. Singleton, Robert L., *Spontaneous flavor and parity breaking with Wilson fermions*, *Phys. Rev.* **D58** (1998) 074501 [hep-lat/9804028] [SPIRES].

JHEP03(2009)006

[33] G. Rupak and N. Shoresh, *Chiral perturbation theory for the Wilson lattice action*, *Phys. Rev.* **D 66** (2002) 054503 [hep-lat/0201019] [SPIRES].

[34] K. Symanzik, *Continuum Limit and Improved Action in Lattice Theories. 1. Principles and ϕ^4 theory*, *Nucl. Phys.* **B 226** (1983) 187 [SPIRES].

[35] K. Symanzik, *Continuum Limit and improved action in lattice theories. 2. $O(N)$ nonlinear σ-model in perturbation theory*, *Nucl. Phys.* **B 226** (1983) 205 [SPIRES].

[36] O. Bär, G. Rupak and N. Shoresh, *Chiral perturbation theory at $O(a^2)$ for lattice QCD*, *Phys. Rev.* **D 70** (2004) 034508 [hep-lat/0306021] [SPIRES].

[37] S. Aoki, *Chiral perturbation theory with Wilson-type fermions including a**2 effects: n(f) = 2 degenerate case*, *Phys. Rev.* **D68** (2003) 054508 [hep-lat/0306027] [SPIRES].

[38] S. Weinberg, *Phenomenological lagrangians*, *Physica* **A 96** (1979) 327 [SPIRES].

[39] S.R. Sharpe and J.M.S. Wu, *Twisted mass chiral perturbation theory at next-to-leading order*, *Phys. Rev.* **D 71** (2005) 074501 [hep-lat/0411021] [SPIRES].

[40] S. Aoki and O. Bär, *The vector and axial vector current in Wilson ChPT*, PoS(LATTICE 2007)062.

[41] S.R. Sharpe and J.M.S. Wu, *The phase diagram of twisted mass lattice QCD*, *Phys. Rev.* **D 70** (2004) 094029 [hep-lat/0407025] [SPIRES].

[42] S. Aoki, O. Bär and B. Biedermann, *Pion scattering in Wilson ChPT*, arXiv:0806.4863 [SPIRES].

[43] S. Aoki, *New phase structure for lattice QCD with wilson fermions*, *Phys. Rev.* **D30** (1984) 2653 [SPIRES].

[44] J. Gasser and H. Leutwyler, *Spontaneously broken symmetries: eeffective lagrangians at finite volume*, *Nucl. Phys.* **B 307** (1988) 763 [SPIRES].

[45] F.C. Hansen, *Finite size effects in spontaneously broken* $\mathrm{SU}(N) \times \mathrm{SU}(N)$ *theories*, *Nucl. Phys.* **B 345** (1990) 685 [SPIRES].

[46] P. Hernández and M. Laine, *Correlators of left charges and weak operators in finite volume chiral perturbation theory*, *JHEP* **01** (2003) 063 [hep-lat/0212014] [SPIRES].

[47] I. Gradshteyn and I. Ryzhik, *Table of integrals, series and products*, 4^{th} edition, Academic PRess, U.S.A. (1983).

[48] P.H. Damgaard, M.C. Diamantini, P. Hernández and K. Jansen, *Finite-size scaling of meson propagators*, *Nucl. Phys.* **B 629** (2002) 445 [hep-lat/0112016] [SPIRES].

[49] P.H. Damgaard, P. Hernández, K. Jansen, M. Laine and L. Lellouch, *Finite-size scaling of vector and axial current correlators*, *Nucl. Phys.* **B 656** (2003) 226 [hep-lat/0211020] [SPIRES].

[50] C. Michael and C. Urbach, *Neutral mesons and disconnected diagrams in twisted mass QCD*, PoS(LATTICE 2007)122.

[51] S. Aoki and O. Bär, *WChPT analysis of twisted mass lattice data*, *Eur. Phys. J.* **A 31** (2007) 481 [hep-lat/0610085] [SPIRES].

[52] A. Hasenfratz, R. Hoffmann and S. Schaefer, *Epsilon regime calculations with reweighted clover fermions*, in the proceedings of *LATTICE 2008*, July 14–19, Williamsburg, Virginia, U.S.A. (2008) [arXiv:0810.0496].

JHEP03(2009)006

[53] A. Hasenfratz, R. Hoffmann and S. Schaefer, *Hypercubic smeared links for dynamical fermions*, *JHEP* **05** (2007) 029 [hep-lat/0702028] [SPIRES].

[54] R. Sommer, *A new way to set the energy scale in lattice gauge theories and its applications to the static force and α_s in* SU(2) *Yang-Mills theory*, *Nucl. Phys.* **B 411** (1994) 839 [hep-lat/9310022] [SPIRES].

[55] F. Bernardoni, P.H. Damgaard, H. Fukaya and P. Hernández, *Finite volume scaling of pseudo Nambu-Goldstone bosons in QCD*, *JHEP* **10** (2008) 008 [arXiv:0808.1986] [SPIRES].

[56] A. Shindler, *Observations on the Wilson fermions in the ϵ-regime*, *Phys. Lett.* **B 672** (2009) 82 [arXiv:0812.2251] [SPIRES].

[57] P. Hasenfratz and H. Leutwyler, *Goldstone boson related finite size effects in field theory and critical phenomena with $O(N)$ symmetry*, *Nucl. Phys.* **B 343** (1990) 241 [SPIRES].

JHEP03(2009)006